Catalysis Today 158 (2010) 475–480

Contents lists available at ScienceDirect

Catalysis Today

journal homepage: www.elsevier.com/locate/cattod

Structural and textural evolution of Ni/γ-Al_2O_3 catalyst under hydrothermal conditions

Haitao Li, Yalin Xu, Chunguang Gao, Yongxiang Zhao *

School of Chemistry and Chemical Engineering, Engineering Research Center of Ministry of Education for Fine Chemicals, Shanxi University, Taiyuan 030006, Shanxi, PR China

ARTICLE INFO

Article history:
Available online 23 August 2010

Keywords:
Hydrothermal treatment
Ni/γ-Al_2O_3 catalyst
Boehmite
Hydration

ABSTRACT

The influence of hydrothermal treatment on the structural and textural properties of Ni/γ-Al_2O_3 catalysts is investigated by means of X-ray diffraction (XRD), H_2-TPR, TG–DSC and N_2 physisorption. After hydrothermally treated at 90–150 °C and 8–48 h, the γ-Al_2O_3 support transforms into its hydrated phase, boehmite [γ-AlO(OH)]. And the content of γ-AlO(OH) increases with the hydrothermal temperature and time increasing. Furthermore, the hydration of γ-Al_2O_3 support induces the aggregation of carried Ni crystallite and decreases the BET specific surface area and pore volume, and also reduces the interaction between Ni and γ-Al_2O_3 support. The above structural and textural changes further cause the hydrogenation activity decay of Ni/γ-Al_2O_3 catalyst.

1. Introduction

Ni/γ-Al_2O_3 catalysts are widely employed in many chemical processes such as hydrogenation, dehydrogenation, reforming, methanation, desulfurization, dechlorination, to produce lots of bulk and fine chemicals [1–6]. During the processes of preparation, storage and usage, the Ni/γ-Al_2O_3 catalysts are generally in contact with water [7]. For instance, these catalysts are generally prepared by impregnation of nickel nitrate aqueous solution on an Al_2O_3 support [8]. The Ni/γ-Al_2O_3 catalysts are often stored in water or humid atmosphere [9]. What is more, these catalysts are even employed in some catalytic reactions in aqueous solution, e.g. industrial production of 1,4-butanediol by Reppe method [10], degradation of oxalic acid [11], hydrogenation of 3-hydroxypropanal [12] and benzophenone [13]. It can be expected, owing to the environmental-friendly nature, nontoxicity, abundance, low cost and so on, water will play an increasingly important role in the development of green chemical industrial processes. Naturally, the influence of water on properties of Ni/γ-Al_2O_3 catalysts is a valuable research point.

It is well known that metal-free γ-Al_2O_3 support can react with water, and transforms gradually into its hydrated phase. Some recent studies have shown that the hydration of γ-Al_2O_3 occurs even at room temperature [7,9,14,15]. Moreover, many researchers have utilized the hydration reaction to modify γ-Al_2O_3 support properties involving pore structure and surface acid–base, and to promote the dispersion of a loaded metal on a γ-Al_2O_3 support [16–20]. For Ni/γ-Al_2O_3 catalysts, Ni species partially occupy the surface tetrahedral or octahedral interstitial sites of γ-Al_2O_3 support, which influence the hydration of γ-Al_2O_3. Meanwhile, the hydration of γ-Al_2O_3 will inevitably change the properties of Ni/γ-Al_2O_3 catalysts, and then affect its activity, selectivity and lifetime. If Ni/γ-Al_2O_3 catalysts are employed in a water containing reaction, the issue is more important. However, the influence of hydration on properties of Ni/γ-Al_2O_3 catalysts is scarcely reported in open literature.

In this work, under hydrothermal conditions, the structural and textural evolution of an industrialized 17 wt% Ni/γ-Al_2O_3 catalyst was investigated. Also, the hydrothermally treated catalysts were employed in the hydrogenation of crude 1,4-butanediol (BDO) aqueous solution, which is a classical reaction under hydrothermal conditions. Effects of hydrothermal treatments on the hydrogenation activity of Ni/γ-Al_2O_3 catalyst were studied. This research is helpful to understand the changes in catalytic performance when the catalysts are employed in a water containing reaction.

2. Experimental

2.1. Catalyst preparation

A Ni/γ-Al_2O_3 catalyst with 17 wt% loading of Ni (HC-08, developed by Shanxi University, has been employed in hydrogenation of crude 1,4-butanediol aqueous solution by Shanxi Sanwei Group Co. Ltd.) was prepared by wet impregnation method, using nickel nitrate salt [$Ni(NO_3)_2{\cdot}6H_2O$] as precursor and a high specific surface area γ-Al_2O_3 (S_{BET} = 310–330 m^2/g) as support. The catalyst was dried at 120 °C for 3 h and calcined at 450 °C for 3 h and then reduced by flowing hydrogen at 450 °C for 2 h.

* Corresponding author. Tel.: +86 351 7011587; fax: +86 351 7011688.
E-mail address: yxzhao@sxu.edu.cn (Y. Zhao).

0920-5861/$ – see front matter © 2010 Elsevier B.V. All rights reserved.
doi:10.1016/j.cattod.2010.07.015

2.2. Hydrothermal treatment of Ni/γ-Al_2O_3 catalyst

The Ni/γ-Al_2O_3 catalyst was hydrothermally treated in a closed stainless steel autoclave reactor with stirring (200 rpm) at various temperatures and times. The hydrothermally treated catalysts were washed with distilled water and then dried at 120 °C in nitrogen before the characterization.

2.3. Hydrogenation activity tests of Ni/γ-Al_2O_3 catalyst

The hydrogenation of crude BDO aqueous solution was performed using a fixed bed reactor (15 mm i.d.). Before the reaction, sample was loaded in the reactor and the feed was pumped continuously into the reactor. And the reaction conditions were as follows T = 393–427 K, P_{H2} = 13 MPa, $LHSV$ = 1.2/h. The feed employed in this study was the product of the first-stage hydrogenation of 1,4-butynediol (BYD) aqueous solution, consisted of 30 wt% BDO, and a minor amount of BYD, 1,4-butenedio (BED), 4-hydroxybutyraldehyde (HBD) and other carbonyl compounds. The carbonyl number of the feed was about 10.6 mg (KOH)/g.

2.4. Catalyst characterization

Powder X-ray diffraction (XRD) was performed using a Bruker D8 Advance X-ray diffractometer with a Cu Kα source at 40 kV and 40 mA. Scanning was carried out over a 2θ range from 10° to 80° at a speed of 6°/min.

N_2 physisorption measurements were performed on a Micromeritics ASAP 2020 instrument. Before measurements, the samples were degassed under vacuum at 120 °C. The specific surface area was calculated using the BET method, and the pore volume and pore size distribution curves were determined from the N_2 desorption isotherm using BJH method.

TG–DSC measurements were carried out using a Netzsch STA 449 thermal analyzer. Samples were heated at a rate of 10 °C/min from room temperature to 800 °C in flowing N_2 (20 mL/min).

TPR experiments were performed in a quartz reactor. The untreated and hydrothermally treated catalysts were calcined at 450 °C in air before the measurements. In a typical experiment, 30 mg of sample (40–60 mesh) was loaded in a quartz reactor, which was placed in a furnace and heated from room temperature to 800 °C with a heating rate of 10 °C/min, and 5% H_2/N_2 with a total flow rate of 20 mL/min was used as a reducing agent. The hydrogen consumption due to the reduction of NiO was detected by a thermal conductivity detector (TCD) and a computer data acquisition system.

3. Results and discussion

3.1. Structural change of Ni/γ-Al_2O_3 catalyst caused by hydrothermal treatment

XRD patterns of the Ni/γ-Al_2O_3 catalysts hydrothermally treated at different temperatures (90 °C, 110 °C, 130 °C, 150 °C) for 8 h are presented in Fig. 1. Compared with the untreated catalyst, a new boehmite [γ-AlO(OH)] phase (2θ = 14.5°, 28.2°, 38.4°, 49.3°, 55.3°, 60.6°, 64.1°, 65.0°, 67.7°, 72.0°) started to appear on the treated catalyst at 110 °C, and its diffraction peak intensity increased with the temperature raising. The result indicated that the support γ-Al_2O_3 partially transformed into γ-AlO(OH), the γ-AlO(OH) content increased and the γ-AlO(OH) phase growth to large grain with the increase in temperature [7]. Another change in XRD patterns is that the intensity of metal Ni diffraction peaks (2θ = 44.5°, 52.0° and 76.5°) was also increased along with the temperature raising. The mean crystallite size of metal Ni were about 6.5 nm, 6.7 nm, 7.0 nm, 7.8 nm and 8.9 nm for the untreated and 90 °C, 110 °C, 130 °C and 150 °C treated catalysts, respectively, which were calculated from line broadening of Ni (2 0 0) diffraction line using the Scherrer equation. The result indicated that the aggregation of Ni crystallite on support occurred during hydrothermal treatment.

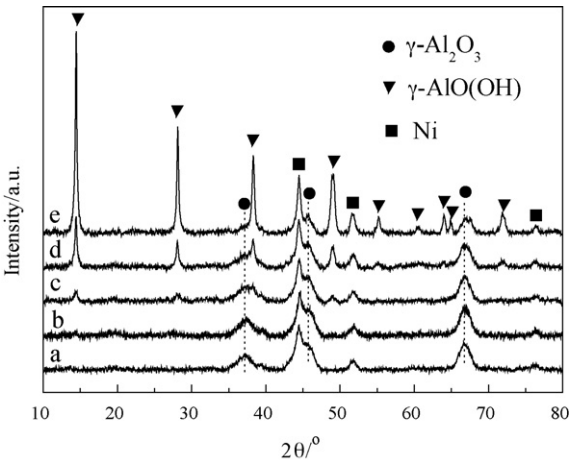

Fig. 1. XRD patterns of Ni/γ-Al_2O_3 catalysts hydrothermally treated for 8 h at different temperature (a) untreated catalyst, (b) 90 °C, (c) 110 °C, (d) 130 °C, and (e) 150 °C.

The XRD patterns of Ni/γ-Al_2O_3 catalysts hydrothermally treated for various times (8 h, 12.5 h, 16 h, 39 h, 48 h) at 110 °C were shown in Fig. 2. The intensity of γ-AlO(OH) and metal Ni diffraction lines increased with the increase in hydrothermal time from 8 h up to 48 h. The trend was similar to that found in Fig. 1.

The transformation of γ-Al_2O_3 into a hydrated phase has already been reported by other researchers, the hydrated species formed during the hydration process varied depending on the medium pH, the temperature and other factors [7,9,14]. Carrier et al. [7] studied the transformation of γ-Al_2O_3 in aqueous suspensions at room temperature and found that the main hydrated phase was gibbsite in the acidic pH range, while the bayerite was predominantly observed at near-neutral pH and higher pH. Rinaldi et al. [9] found that γ-AlO(OH) phase was observed during the hydration of alumina calcined at 200–500 °C, and the bayerite phase appeared for the alumina calcined at 400–1000 °C. Absi-Halabi et al. [16] reported that γ-Al_2O_3 transformed into γ-AlO(OH) in the presence of water vapor in the temperature range of 150–300 °C. In the present study, the γ-Al_2O_3 support in Ni/γ-Al_2O_3 catalyst also transformed into γ-AlO(OH) phase after the hydrothermal treat-

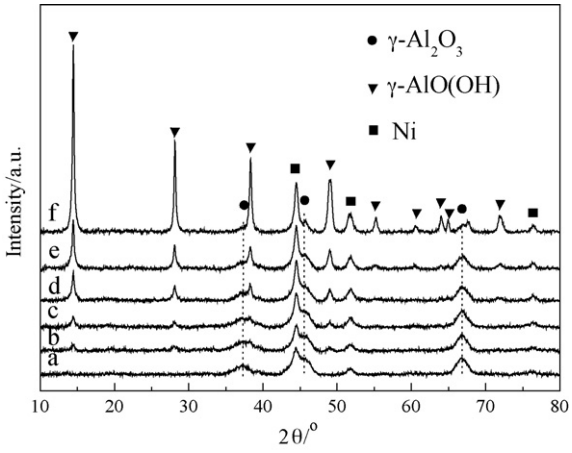

Fig. 2. XRD patterns of Ni/γ-Al_2O_3 catalysts hydrothermally treated at 110 °C for different time (a) untreated catalyst, (b) 8 h, (c) 12.5 h, (d) 16 h, (e) 39 h, and (f) 48 h.

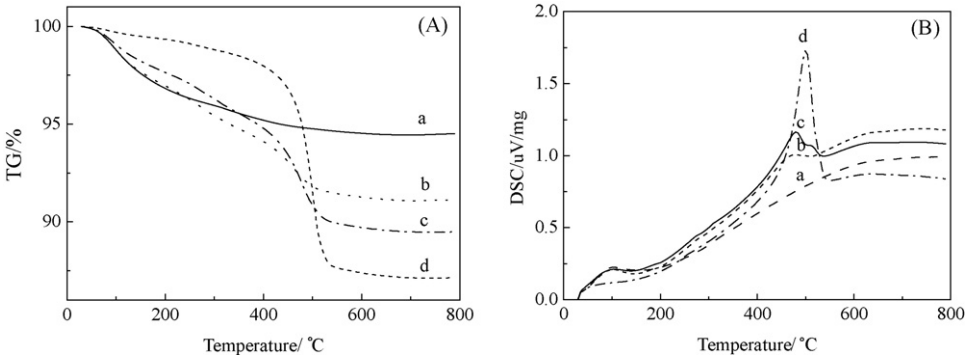

Fig. 3. TG–DSC profiles (A: TG curves; B: DSC curves) of Ni/γ-Al_2O_3 catalysts hydrothermally treated at 110 °C for different times (a) untreated catalyst, (b) 8 h, (c) 16 h, and (d) 48 h.

ment in the temperature range of 110–150 °C, and the presence of metal Ni did not change the property of γ-Al_2O_3 hydration remarkably.

Also, the aggregation of Ni on supports has been widely reported, which is generally driven by temperature and unlikely occurs when temperature is below 200 °C [21–23]. But in the present work, the supported Ni species was aggregated obviously at temperature range of 110–150 °C in the hydrothermal conditions. Thus, it can be supposed that the aggregation of metal Ni should not be mainly caused by the temperature driven migration and coalescence. Considering that the mean metal Ni crystallite size and the γ-AlO(OH) content are increasing simultaneously, we speculated that the aggregation of metal Ni on the surface of γ-Al_2O_3 support is caused by the transformation of γ-Al_2O_3 into γ-AlO(OH).

3.2. Quantification of hydrated phase

TG–DSC curves of the Ni/γ-Al_2O_3 catalysts hydrothermally treated at different times are presented in Fig. 3. For the untreated Ni/γ-Al_2O_3 catalyst, a 2.90 wt% mass-loss stage (from room temperature to 210 °C) in the TG curve accompanied with an endothermic peak at 100 °C in the DSC curve can be seen, which should be attributed to the desorption of physically adsorbed water [14]. The mass loss above 210 °C was owing to the removal of surface hydroxyl. For the hydrothermally treated samples, the TG curves can be divided into three stages. The first stage (from room temperature to 210 °C), corresponding to an endothermic peak at 100 °C in the DSC curve, was attributed to the desorption of physically adsorbed water, the second stage (from 210 °C to 400 °C) to the removal of surface hydroxyl, and the third one (from 400 °C to about 560 °C), corresponding to one or two endothermic peaks in the DSC curve, to the dehydration of γ-AlO(OH) as the following reaction [7]:

$$2\gamma\text{-AlO(OH)} \rightarrow \gamma\text{-}Al_2O_3 + H_2O.$$

Thus, the γ-AlO(OH) content in the hydrothermally treated samples can be calculated according to the following equation:

$$\%_{\gamma\text{-AlO(OH)}} = \frac{\%_{H_2O}}{M_{H_2O}} \times 2 \times M_{\gamma\text{-AlO(OH)}}$$

where $\%_{H_2O}$ is the mass loss between 400 °C and 560 °C, 2 is the stoichiometric factor, i.e. γ-AlO(OH)/H_2O ratio in the reaction, M_{H_2O} and $M_{\gamma\text{-AlO(OH)}}$ are molecular weight of H_2O and γ-AlO(OH), respectively. As shown in Table 1, the γ-AlO(OH) contents were 18.2%, 32.7% and 69.3% for the 8 h, 16 h and 48 h hydrothermally treated samples, respectively.

Evolution of mass loss for various temperature stages in the TG curves with increasing hydrothermal time is shown in Fig. 4. It can be seen, after 8 h hydrothermal treatment, the mass loss in the first

Table 1
Textural properties of Ni/γ-Al_2O_3 catalysts.

Hydrothermal time (h)	Specific surface area (m^2/g)	Pore volume (cm^3/g)	Average pore diameter (nm)	γ-AlO(OH) content (%)
Fresh	285	0.65	9.17	–
8	150	0.44	11.63	18.2
16	98	0.36	14.58	32.7
48	25	0.16	24.65	69.3

(below 210 °C) temperature stage in the TG curve had a decrease, while the mass loss in both of the second (210–400 °C) and third (from 400 °C to about 560 °C) temperature stages in the TG curves increased. The results indicated that the physically adsorbed water transformed into surface hydroxyl and hydroxyl in γ-AlO(OH) lattice. With the further increase in hydrothermal treatment time, the mass loss caused by the removal of physically adsorbed water and surface hydroxyl decreased, while the mass loss caused by the dehydration of γ-AlO(OH) phase increased. Indicating that both of the physically adsorbed water and surface hydroxyl finally transformed into hydroxyl in γ-AlO(OH) lattice. The surface hydroxyl can be considered as a intermediate state during the transformation of physically adsorbed water into hydroxyl in γ-AlO(OH) lattice. Thus, according to the TG–DSC results, the hydration of γ-Al_2O_3 support may involve the following steps:

(i) the physically adsorbed water increased on the Ni/γ-Al_2O_3 catalyst,
(ii) the physically adsorbed water transformed into surface hydroxyl,

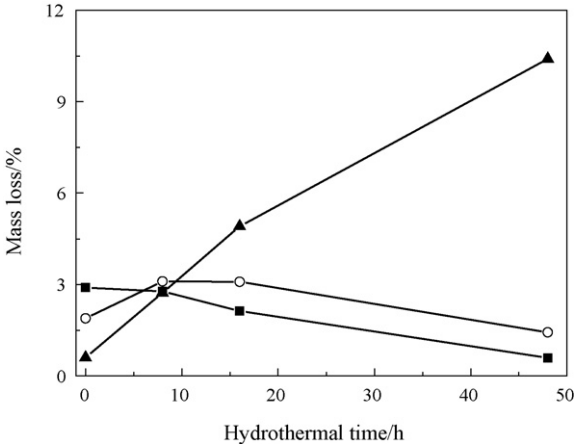

Fig. 4. Evolution of mass loss below 210 °C (■) and from 210 °C to 400 °C (○) and from 400 °C to 560 °C (▲) measured by TG as increasing hydrothermal time.

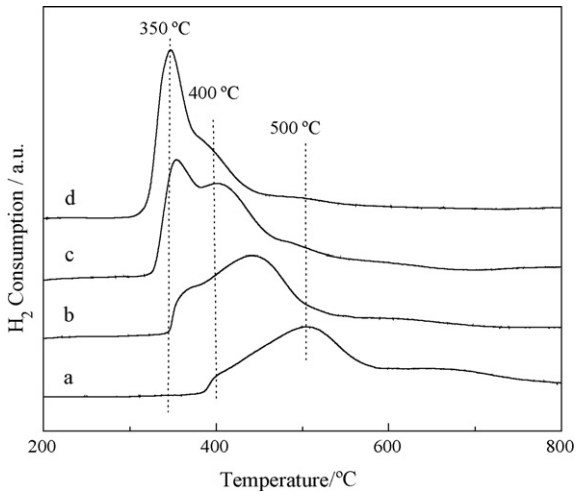

Fig. 5. TPR profiles of Ni/γ-Al_2O_3 catalysts hydrothermally treated at 110 °C for different times (a) untreated catalyst, (b) 8 h, (c) 16 h, and (d) 48 h.

(iii) the γ-AlO(OH) phase formed and increased with the hydrothermal time increasing.

3.3. Change of metal–support interaction caused by hydrothermal treatment

The influence of hydrothermal treatment on Ni–support interaction in the Ni/γ-Al_2O_3 catalyst was investigated by TPR experiments. It is known that supported nickel catalysts show different reduction behavior depending on the nature of nickel–support interaction, bulk nickel oxide that weakly interact with support is reduced around 350–400 °C, when nickel is highly dispersed on Al_2O_3, the metal–support interaction decreases the reducibility of the nickel ion to Ni^0 and its reduction peak appears above 500 °C [24,25]. As shown in Fig. 5, all samples showed two reduction peaks. The untreated catalyst exhibited a broad high temperature reduction peak around 500 °C with a little shoulder at 400 °C, indicating that the Ni species mainly existed as highly dispersed NiO crystallite having strong interaction with support [26–28]. For the hydrothermally treated samples, both of the reduction peaks shifted to lower temperature and the fraction of the lower temperature peak increased with increasing hydrothermal time from 8 h to 48 h. The result indicated that the interaction between Ni and support γ-Al_2O_3 was weakened during the hydrothermal process [29,30].

The interaction between nickel and γ-Al_2O_3 has been widely studied [31]. Many studies show that the metal–support interaction in Ni/γ-Al_2O_3 catalyst is related to the medium-strong and strong Lewis acid sites of γ-Al_2O_3, the higher the content of medium-strong and strong Lewis acid sites, the stronger the interaction between Ni^{2+} and γ-Al_2O_3 [32–34]. Liu [34] found that the hydration of γ-Al_2O_3 occurs preferentially on the medium-strong and strong Lewis acid sites, i.e. the contents of the medium-strong and strong Lewis acid sites decrease after hydration. Thus, for the Ni/γ-Al_2O_3 catalyst, the hydration of γ-Al_2O_3 support may result in the decrease of medium-strong and strong Lewis acid sites, which should be one of the reasons for the weakening of Ni–support interaction. In addition, it was also reported that the smaller the Ni crystallite sizes, the higher the maximum temperature of reduction, i.e. the stronger the interaction between Ni and support [30,35]. Thus, the growth of Ni crystallite sizes, which was observed by XRD, may be another reason for the weakening of Ni–support interaction.

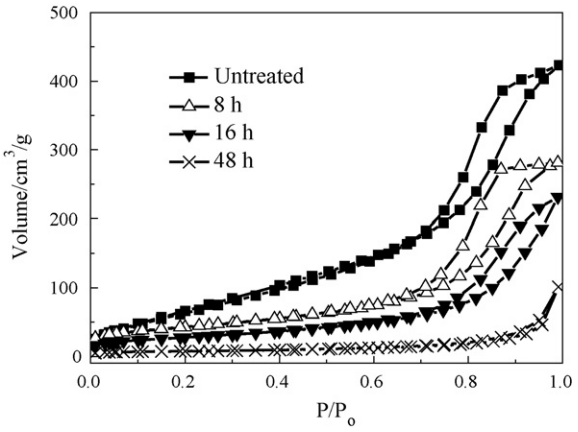

Fig. 6. N_2 adsorption–desorption isotherms of Ni/γ-Al_2O_3 catalysts.

3.4. Textural change of Ni/γ-Al_2O_3 catalyst caused by hydrothermal treatment

The N_2 physisorption isotherms of the untreated and hydrothermally treated Ni/γ-Al_2O_3 catalysts are shown in Fig. 6. All the isotherms are of type-IV, characteristic of mesoporous structure with the hysteresis loops, but the patterns of the hysteresis loops were different. According to de Boer's theory, the loop of the untreated and 8 h hydrothermally treated catalysts were of type B associated with capillary condensation in slit-shape mesopore, whereas the loop of the 48 h hydrothermally treated sample was of type A associated with capillary condensation in cylinder-shape mesopore. The loop of the 16 h hydrothermally treated sample seemed to be the combination of both types. Thus, the mesoporous structure of Ni/γ-Al_2O_3 catalyst transformed from type B to type A during the hydrothermal treatment.

Table 1 summarizes some textural properties of the untreated and hydrothermally treated catalysts, and the pore size distributions are shown in Fig. 7. The BET specific surface area of the untreated catalyst was 285 m^2/g. And the pore volume and mean pore diameter of the untreated catalyst were 0.65 cm^3/g and 9.17 nm, respectively. After hydrothermal treatment, the BET specific surface area and pore volume of the catalyst decreased remarkably, however, the mean pore diameter increased with the increase in hydrothermal time. As shown in Fig. 7, the primary mesopore peak for the untreated sample was around 5–20 nm, accompanied with a secondary peak of 2–4 nm. For the 8 h hydrothermally treated sample, the small pores less than 4 nm disappeared and only one mesopore peak between 5 nm and 20 nm

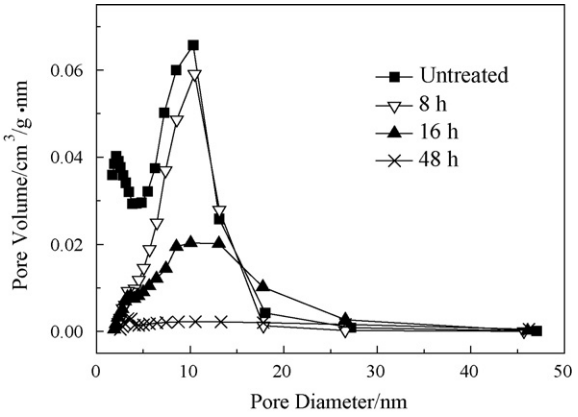

Fig. 7. Pore size distribution curves of Ni/γ-Al_2O_3 catalysts.

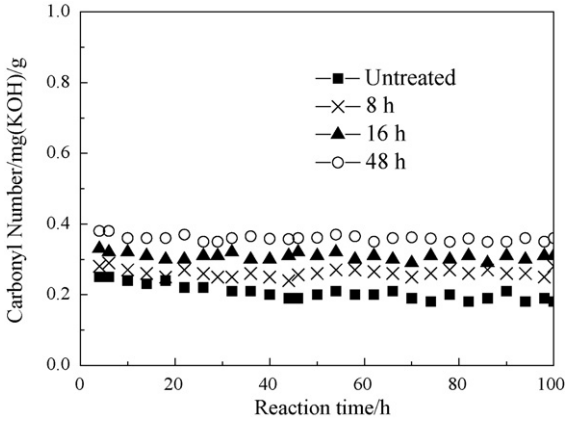

Fig. 8. Activity tests of Ni/γ-Al_2O_3 catalysts. (*Reaction conditions*: T = 393 K, P_{H2} = 13 MPa, *LHSV* = 1.2/h, feed carbonyl number 10.6 mg (KOH)/g.)

was found. With the further increase in hydrothermal time, the primary mesopore peaks around 5 nm and 20 nm decreased. For the 48 h hydrothermally treated sample, the primary mesopore peaks around 5 nm and 20 nm almost disappeared. It is well known the growth of primary crystals can cause the decrease in pore volume and specific surface area of Al_2O_3 [16]. Thus, above textural changes of the Ni/γ-Al_2O_3 catalyst should be mainly attribute to the formation and growth of boehmite crystals during the hydrothermal treatment.

3.5. Activity tests of Ni/γ-Al_2O_3 catalysts hydrothermally treated for various times

The results for the liquid phase hydrogenation of crude BDO over the untreated and hydrothermally treated Ni/γ-Al_2O_3 catalysts are shown in Fig. 8. The aim of the reaction is the hydrogenation of BYD, BED, HBD and other carbonyl compounds. It is well known that the hydrogenation of C=O is more difficult than C≡C and C=C. Thus, in industrial process, the contents of carbonyl compounds in the hydrogenation product are the main concern for this reaction. However, the contents of carbonyl compounds in the crude BDO solution are low, and the components are very complicated. Consequently, it is difficult to quantify the content of every carbonyl compounds by GC or GC–MS methods, while the chemical titration is a suitable method and has been widely used in industrial process [36]. The principle of chemical titration is that the carbonyl C=O reacts with hydroxylamine hydrochloride, releasing hydrogen chloride. And then the hydrogen chloride is titrated with potassium hydroxide. The equations are as follows:

$$RCOR + NH_2OH{\cdot}HCl \rightarrow R_2C{=}NOH + HCl + H_2O \quad (1)$$

$$HCl + KOH \rightarrow H_2O + KCl \quad (2)$$

Thus, the carbonyl number of the crude BDO solution is calculated according to the following equation:

$$N_{C=O} = X \times 56.1 \times \frac{0.1}{W}$$

where $N_{C=O}$ is the carbonyl number, X is the consumption volume of KOH solution, 56.1 is the molecular weight of KOH, 0.1 is the molar concentration of KOH solution. Therefore, the carbonyl number of crude BDO solution after hydrogenation reaction is the main basis for measuring the effects of hydrogenation, i.e. the activity of Ni/γ-Al_2O_3 catalyst, the lower the carbonyl number, the higher the activity of the Ni/γ-Al_2O_3 catalyst. As shown in Fig. 8, the carbonyl number of the product for untreated Ni/γ-Al_2O_3 catalyst was about 0.2 mg (KOH)/g. After hydrothermal treatment for the Ni/γ-Al_2O_3 catalyst, the carbonyl number increased obviously. For the 48 h hydrothermally treated Ni/γ-Al_2O_3 catalyst, the carbonyl number increased to about 0.38 mg (KOH)/g, indicating that the catalyst showed distinctly activity decay after hydrothermal treatment.

According to above characterization results, the hydrothermal treatment resulted in the hydration of γ-Al_2O_3 support, which further induced the metal Ni crystallite aggregation, the increase of average pore diameter, and the decrease of BET specific surface area and pore volume for the Ni/γ-Al_2O_3 catalyst. It is well known that the aggregation of metal component and the decrease of specific surface area result in the loss of active surface area [21]. And the reduction of the pore diameter increases the internal diffusion resistance. Thus, all above structural and textural changes caused the activity decay of Ni/γ-Al_2O_3 catalyst during the hydrothermal treatment. And the hydration of γ-Al_2O_3 is considered the essential reason.

4. Conclusions

Under hydrothermal conditions, the structural and textural properties of Ni/γ-Al_2O_3 catalyst are changed. The γ-Al_2O_3 support transforms into γ-AlO(OH) partially, and the presence of Ni does not affect obviously the hydration of γ-Al_2O_3 support. It can be supposed that the hydration of γ-Al_2O_3 support involves the following three steps: firstly, the water is physically adsorbed on the Ni/γ-Al_2O_3 catalyst surface, and then the adsorbed water reacts with γ-Al_2O_3, thirdly the γ-AlO(OH) phase forms and its content increases with the increase in hydrothermal time. It is also found that the formation and growth of γ-AlO(OH) crystal phase result in the increase of average pore diameter, the decrease of BET specific surface area and pore volume, and the aggregation of metal Ni. In addition, the hydration of γ-Al_2O_3 support further results in the reduction of the metal–support interaction. The above structural and textural changes also caused the activity decay of Ni/γ-Al_2O_3 catalyst employed in hydrogenation of crude BDO aqueous solution.

Acknowledgments

The authors gratefully acknowledge financial support from The National High Technology Research and Development Program of China (2005AA001050), The National Natural Science Foundation of China (20573071), Scientific and Technological Project of Shanxi Province (20080321017) and Shanxi Programs for Science and Technology Innovation (2007101008).

References

[1] P.G. Savva, K. Goundani, J. Vakros, K. Bourikas, C. Fountzoula, D. Vattis, A. Lycourghiotis, C. Kordulis, Benzene hydrogenation over Ni/Al_2O_3 catalysts prepared by conventional and sol–gel techniques, Appl. Catal. B 79 (2008) 199–207.
[2] S. Yolcular, Ö. Olgun, Ni/Al_2O_3 catalysts and their activity in dehydrogenation of methylcyclohexane for hydrogen production, Catal. Today 138 (2008) 198–202.
[3] A.S.A. Al-Fatish, A.A. Ibrahim, A.H. Fakeeha, M.A. Soliman, M.R.H. Siddiqui, A.E. Abasaeed, Coke formation during CO_2 reforming of CH_4 over alumina-supported nickel catalysts, Appl. Catal. A 364 (2009) 150–155.
[4] A.E. Aksoylu, Z.İ. Onsan, Hydrogenation of carbon oxides using coprecipitated and impregnated Ni/A1$_2O_3$ catalysts, Appl. Catal. A 164 (1997) 1–11.
[5] A.R. Suzdorf, S.V. Morozov, N.N. Anshits, S.I. Tsignova, A.G. Anshits, Gas phase hydrodechlorination of chlorinated aromatic compounds on nickel catalysts, Catal. Lett. 29 (1994) 49–55.
[6] S. Hernández, L. Solarino, G. Orsello, N. Russo, D. Fino, G. Saracco, V. Specchia, Desulfurization processes for fuel cells systems, Int. J. Hydrogen Energy 33 (2008) 3209–3214.
[7] X. Carrier, E. Marceau, J.F. Lambert, M. Che, Transformations of γ-alumina in aqueous suspensions 1. Alumina chemical weathering studied as a function of pH, J. Colloid Interface Sci. 308 (2007) 429–437.
[8] S. Velu, S.K. Gangwal, Synthesis of alumina supported nickel nanoparticle catalysts and evaluation of nickel metal dispersions by temperature programmed desorption, Solid State Ionics 177 (2006) 803–811.

[9] R. Rinaldi, F.Y. Fujiwara, U. Schuchardt, Structural, morphological and acidic changes of nanocrystalline aluminas caused by a controlled humidity atmosphere, Appl. Catal. A 315 (2006) 44–51.
[10] G.X. Bai, F.X. Huang, H.F. Xu, R.X. Ma, J.B. Zhou, CN Patent 92,105,441.6 (1994).
[11] S.M. Avramescu, C. Bradu, I. Udrea, N. Mihalache, F. Ruta, Degradation of oxalic acid from aqueous solutions by ozonation in presence of Ni/Al_2O_3 catalysts, Catal. Commun. 9 (2008) 2386–2391.
[12] X. Zhu, H. Hofmann, Hydrogenation of 3-hydroxypropanal in trickle beds experimental and modelling, Chem. Eng. Technol. 20 (1997) 131–137.
[13] P.S. Kumbhar, R.A. Rajadhyaksha, Liquid phase catalytic hydrogenation of benzophenone: role of metal support interaction, bimetallic catalysts, solvents and additives, Stud. Surf. Sci. Catal. 78 (1993) 251–258.
[14] G. Lefèvre, M. Duc, P. Lepeut, R. Caplain, M. Fédoroff, Hydration of γ-alumina in water and its effects on surface reactivity, Langmuir 18 (2002) 7530–7537.
[15] E. Laiti, P. Persson, L.O. Öhman, Balance between surface complexation and surface phase transformation at the alumina/water interface, Langmuir 14 (1998) 825–831.
[16] M. Absi-Halabi, A. Stanislaus, H. Al-Zaid, Effect of acidic and basic vapors on pore size distribution of alumina under hydrothermal conditions, Appl. Catal. A 101 (1993) 117–128.
[17] A. Stanislaus, K. Al-Dolama, M. Absi-Halabi, Preparation of a large pore alumina-based HDM catalyst by hydrothermal treatment and studies on pore enlargement mechanism, J. Mol. Catal. A 181 (2002) 33–39.
[18] J.L. Zhang, J.G. Chen, J. Ren, Y.H. Sun, Chemical treatment of γ-Al_2O_3 and its influence on the properties of Co-based catalysts for Fischer–Tropsch synthesis, Appl. Catal. A 243 (2003) 121–133.
[19] J.C. Li, L. Xiang, X. Feng, Z.W. Wang, F. Wei, Effect of hydrothermal treatment on the acidity distribution of γ-Al_2O_3 support, Appl. Surf. Sci. 253 (2006) 766–770.
[20] J. Li, L. Xiang, X. Feng, Z. Wang, Influence of hydrothermally modified γ-Al_2O_3 on the properties of NiMo/γ-Al_2O_3 catalyst, Appl. Surf. Sci. 254 (2008) 2077–2080.
[21] M. Besson, P. Gallezot, Deactivation of metal catalysts in liquid phase organic reactions, Catal. Today 81 (2003) 547–559.
[22] D.Z. Xiao, H. Hofmann, Deactivation of $Ni/SiO_2/A1_2O_3$-catalyst in hydrogenation of 3-hydroxypropanal solution, Appl. Catal. A 155 (1997) 179–194.
[23] L. Zhao, J.X. Chen, J.Y. Zhang, Deactivation of Ni/K_2O-La_2O_3-SiO_2 catalyst in hydrogenation of *m*-dinitrobenzene to *m*-phenylenediamine, J. Mol. Catal. A: Chem. 246 (2006) 140–145.
[24] K.V.R. Chary, P.V.R. Rao, V.V. Rao, Catalytic functionalities of nickel supported on different polymorphs of alumina, Catal. Commun. 9 (2008) 886–893.
[25] P. Kim, H. Kim, J.B. Joo, W. Kim, I.K. Song, J. Yi, Effect of nickel precursor on the catalytic performance of Ni/Al_2O_3 catalysts in the hydrodechlorination of 1,1,2-trichloroethane, J. Mol. Catal. A: Chem. 256 (2006) 178–183.
[26] L. Zhang, X. Wang, B. Tan, U.S. Ozkan, Effect of preparation method on structural characteristics and propane steam reforming performance of Ni-Al_2O_3 catalysts, J. Mol. Catal. A: Chem. 297 (2009) 26–34.
[27] E. Heracleous, A.F. Lee, K. Wilson, A.A. Lemonidou, Investigation of Ni-based alumina-supported catalysts for the oxidative dehydrogenation of ethane to ethylene: structural characterization and reactivity studies, J. Catal. 231 (2005) 159–171.
[28] A.L. Alberton, M.M.V.M. Souza, M. Schmal, Carbon formation and its influence on ethanol steam reforming over Ni/Al_2O_3 catalysts, Catal. Today 123 (2007) 257–264.
[29] D. Chen, K.O. Christensen, E.O. Fernández, Z. Yu, B. Tøtdal, N. Latorre, A. Monzón, A. Holmen, Synthesis of carbon nanofibers: effects of Ni crystal size during methane decomposition, J. Catal. 229 (2005) 82–96.
[30] J. Ashok, G. Raju, P.S. Reddy, M. Subrahmanyam, A. Venugopal, Catalytic decomposition of CH_4 over NiO-Al_2O_3-SiO_2 catalysts: influence of catalyst preparation conditions on the production of H_2, Int. J. Hydrogen Energy 33 (2008) 4809–4818.
[31] A.N. Kharat, P. Pendleton, A. Badalyan, M. Abedini, M.M. Amini, Decomposition of nickel formate on sol–gel alumina and characterization of product by X-ray photoelectron and TOF-SIMS spectroscopies, J. Catal. 205 (2002) 7–15.
[32] E. Kiš, R. Marinković-Nedučin, G. Lomić, G. Bošković, D.Ž. Obadović, J. Kiurski, P. Putanov, Structural and textural properties of the NiO-Al_2O_3 catalyst, Polyhedron 17 (1998) 27–34.
[33] J. Sehested, J.A.P. Gelten, S. Helveg, Sintering of nickel catalysts: effects of time, atmosphere, temperature, nickel–carrier interactions, and dopants, Appl. Catal. A 309 (2006) 237–246.
[34] X. Liu, DRIFTS study of surface of γ-alumina and its dehydroxylation, J. Phys. Chem. C 112 (2008) 5066–5073.
[35] D. Chen, K.O. Christensen, E.O. Fernández, Z. Yu, B. Tøtdal, N. Latorre, A. Monzó, A. Holmen, Synthesis of carbon nanofibers: effects of Ni crystal size during methane decomposition, J. Catal. 229 (2005) 82–96.
[36] GB 6324.5-86, Organic Chemical Products for Industrial Use-determination of Content of Carbonyl Compounds Present-Volumetric Method.